Hindawi
International Journal of Polymer Science
Volume 2022, Article ID 4761481, 8 pages
https://doi.org/10.1155/2022/4761481

Research Article

Investigation of Mechanical Properties of FDM-Processed *Acacia concinna*–Filled Polylactic Acid Filament

S. Muthu Natarajan, S. Senthil, and P. Narayanasamy

Department of Mechanical Engineering, Kamaraj College of Engineering and Technology, Near Virudhunagar, Madurai, 625 701 Tamil Nadu, India

Correspondence should be addressed to S. Muthu Natarajan; smnrajan25@gmail.com

Received 6 July 2022; Accepted 6 August 2022; Published 12 September 2022

Academic Editor: Joanna Rydz

In this work, an *Acacia concinna* filler was blended in a polylactic acid matrix using a single-screw extruder. A composite filament material made from an extruder was used to fabricate polylactic acid/25 wt% *A. concinna* (PLA/25 wt% AC) composites via a fused deposition modeling (FDM) technique. Composites were fabricated by varying layer thickness, infill density, and printing speed based on Taguchi L9 experimental design. Tensile, flexural, and impact tests were conducted on the printed composite samples as per the ASTM standards. The significance of factors impacting the mechanical properties was determined using analysis of variance. To estimate the strength of PLA/AC composites, mathematical models were developed. In addition, the fractured specimen was examined using scanning electron microscopy to determine the mechanism of fracture. Both the layer height and the infill percentage exhibited a positive influence on strength, which suggests that the layer height or the infill percentage, or both, will increase the material's strength. The printing speed had a negative influence on the strength, which indicates that the strength decreases as the printing speed increases. The findings suggested that PLA/AC composites could be used to fabricate high-strength, lightweight components using FDM.

1. Introduction

Additive manufacturing provides numerous advantages, including the capacity to rapidly prototype complicated structures, mass customization, and the reduction of waste [1]. Additive manufacturing has found widespread application in a variety of sectors, including building construction, prototyping, and biomechanics. 3D printing is one type of additive manufacturing process that can be used to create more varieties of complex structures and geometries from data that come from 3D models [2]. Fused deposition modeling (FDM), also known as additive manufacturing, is becoming an increasingly popular method for the production of polymer-based materials [3]. The FDM process is the most common type of 3D printing technique that is gaining interest because of its low cost, minimal material consumption, and simplicity [4, 5]. Polymer structures created by additive manufacturing methods have low mechanical strength due to low stiffness. Most 3D-printed polymer goods cannot be used as functional components due to the low strength of pure polymer products generated by FDM [6]. There have been numerous attempts to improve the mechanical performance of these printed parts.

Polymer composites prepared using additive manufacturing have eliminated these restrictions by incorporating fibers or fillers, producing fiber-reinforced polymer composites (FRPCs), which are high-performance materials because of their functionality [7, 8]. Because of their superior mechanical characteristics (high strength-to-weight ratio), FRPCs have seen widespread application across a wide range of industries, including the textiles, automotive, and aerospace sectors [7, 9].

The processability and mechanical behavior of FDM-fabricated Acrylonitrile Butadiene Styrene (ABS)-short carbon fiber composites and their applications are discussed [10]. The fused filament fabrication method was used to produce PLA/short-carbon fiber composites [11]. These studies show that these methods can make the composites less tough

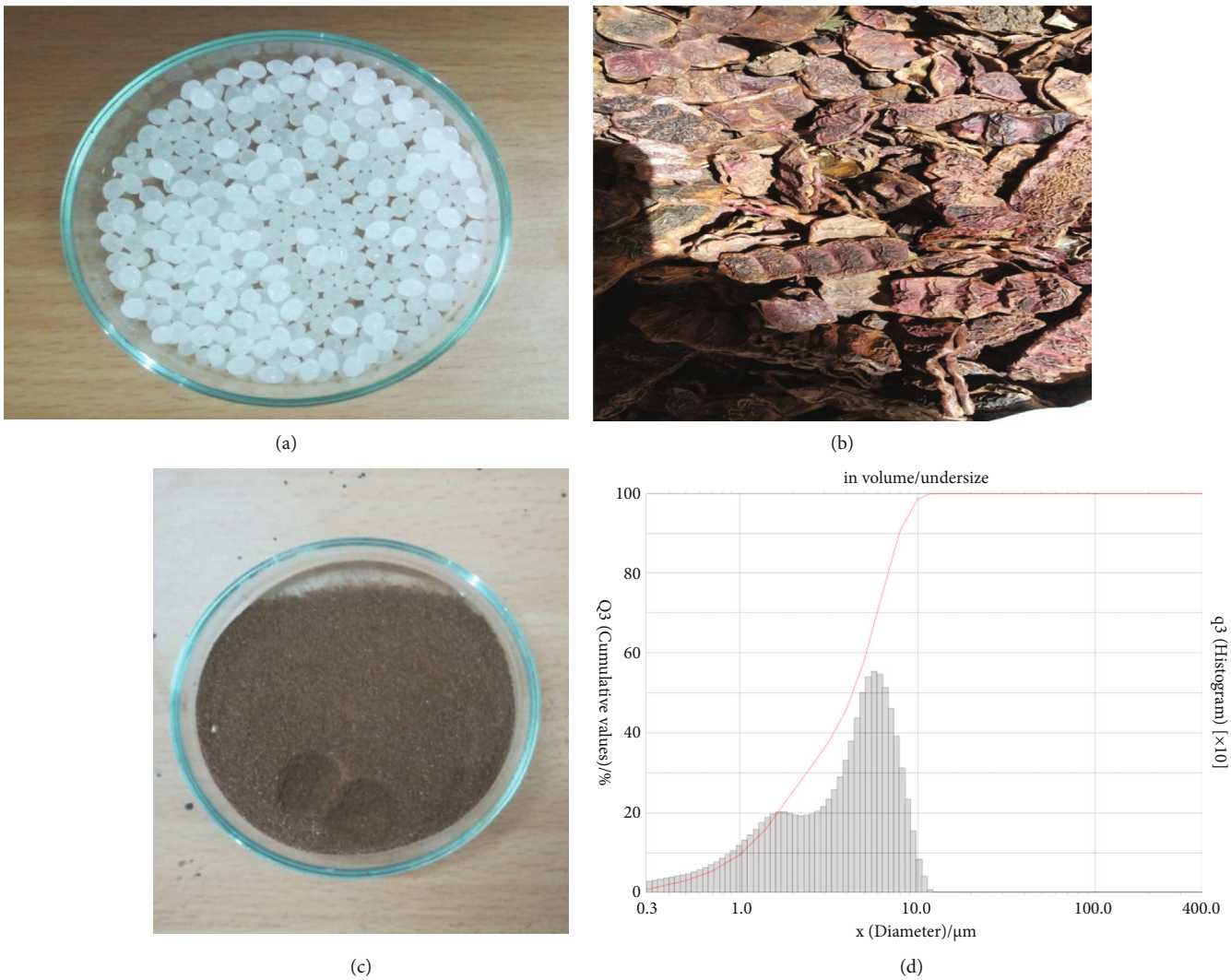

Figure 1: (a) PLA granules, (b) *A. concinna* (AC), (c) pulverized ACF, and (d) particle size of the ACFs.

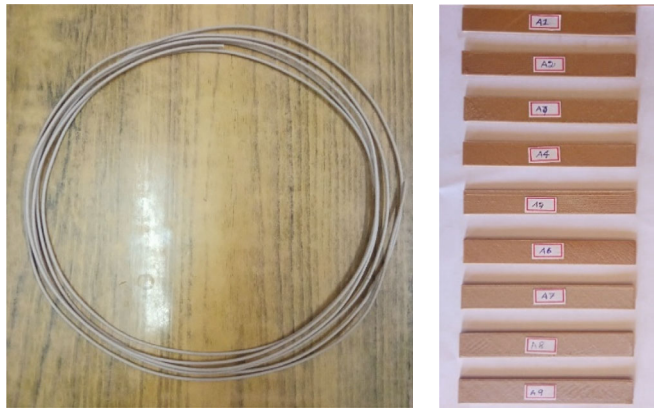

Figure 2: (a) Filament of PLA/25% ACF extrudate of diameter 1.75 mm, and (b) FDM-fabricated PLA/25 wt% ACF composite specimens.

Table 1: Input parameters and their corresponding level values.

Parameters	Units	Level I	Level II	Level III
Layer thickness	mm	0.08	0.16	0.24
Infill density	%	60	80	100
Printing speed	mm/s	50	70	90

Table 2: Experimental results.

Sample no.	Layer height (mm)	Infill percentage	Print speed (mm/s)	Tensile strength (MPa)	Flexural strength (MPa)	Impact strength (kJ/m^2)
1	0.08	60	50	27.69	40.23	15.5933
2	0.08	80	70	24.56	36.58	15.4789
3	0.08	100	90	22.73	35.56	15.3463
4	0.16	60	70	25.72	40.65	16.0165
5	0.16	80	90	23.34	37.50	15.2082
6	0.16	100	50	33.72	46.61	16.6690
7	0.24	60	90	24.10	35.97	15.1565
8	0.24	80	50	30.42	45.22	16.5670
9	0.24	100	70	28.61	43.97	16.2830

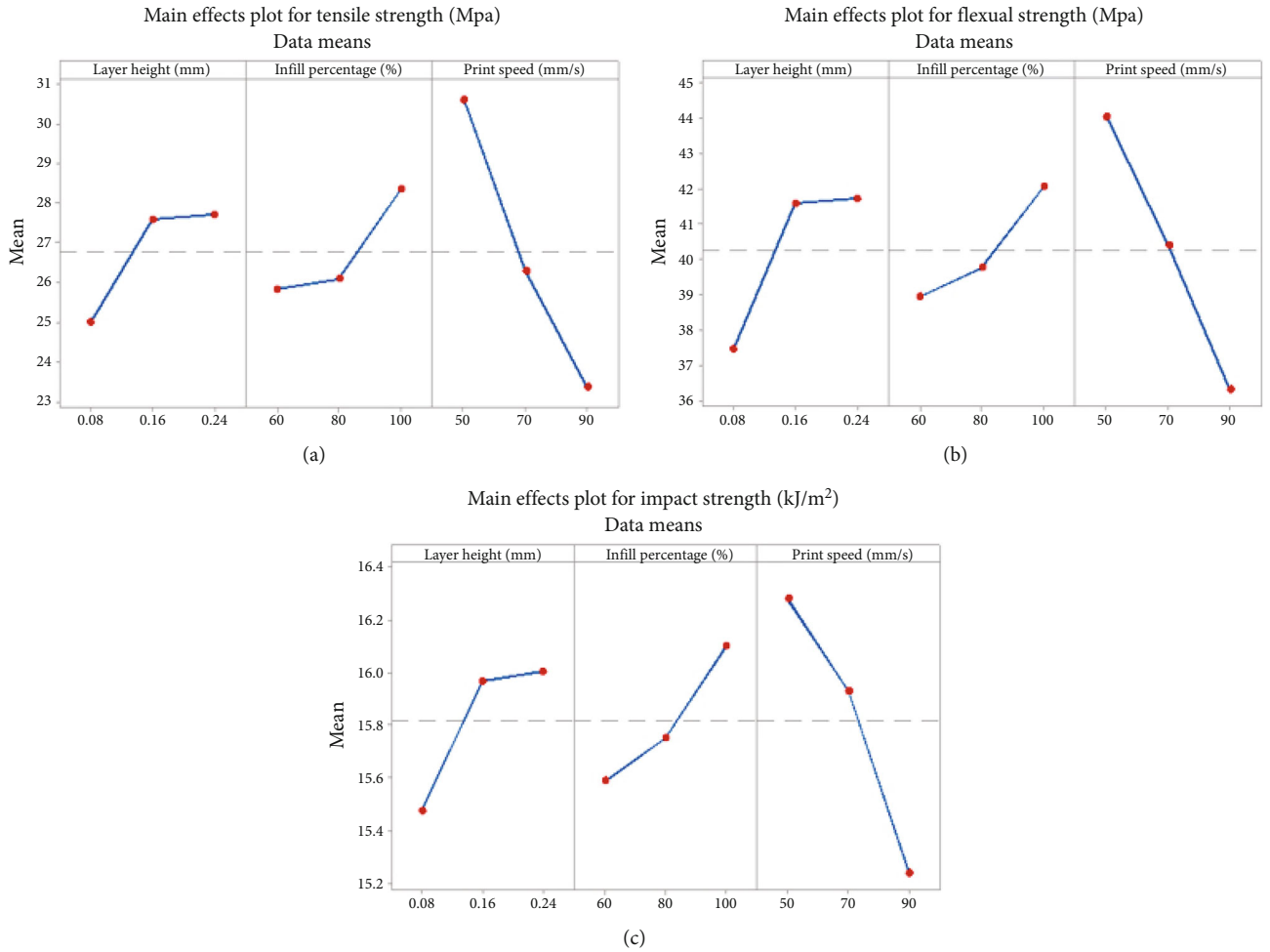

Figure 3: Main effect plot for (a) tensile strength, (b) flexural strength, and (c) impact strength.

Table 3: Analysis of variance for tensile strength.

Source	DF	Adj SS	Adj MS	*F*-Value	*p*-Value	%Contribution
Layer height (mm)	1	11.070	11.070	6.67	0.049	10.34
Infill percentage	1	9.500	9.500	5.73	0.062	8.87
Print speed (mm/s)	1	78.193	78.193	47.13	0.001	73.04
Error	5	8.295	1.659			7.74
Total	8	107.059				

$S = 1.28805$, $R^2 = 92.25\%$, R^2 (adj) = 87.60%.

Table 4: Analysis of variance for flexural strength.

Source	DF	Adj SS	Adj MS	*F*-Value	*p*-Value	%Contribution
Layer height (mm)	1	27.26	27.264	13.04	0.015	19.40
Infill percentage	1	14.38	14.384	6.88	0.047	10.23
Print speed (mm/s)	1	88.40	88.397	42.29	0.001	62.92
Error	5	10.45	2.090			7.43
Total	8	140.50				

$S = 1.44570$, $R^2 = 92.56\%$, R^2(adj) = 88.10%.

Table 5: Analysis of variance for impact strength.

Source	DF	Adj SS	Adj MS	*F*-Value	*p*-Value	%Contribution
Layer height (mm)	1	0.4203	0.42029	6.87	0.047	15.35
Infill percentage	1	0.3912	0.39117	6.39	0.053	14.29
Print speed (mm/s)	1	1.6206	1.62063	26.49	0.004	59.19
Error	5	0.3059	0.06119			11.17
Total	8	2.7380				

$S = 0.247364$, $R^2 = 88.83\%$, R^2 (adj) = 82.12%.

and strong, but they will make them more tensile and flexible. Despite the fact that research on the natural fiber-reinforced polymer is continually expanding, very few studies relating to the FDM of polymer/natural fibers have been conducted [12]. To reduce the cost of FDM printing, a new rice straw–reinforced ABS composite filament was created and its mechanical properties were tested [13].

Typical applications for PLA include products that need both good mechanical qualities and the capacity to degrade, but the cost of the PLA is quite high. Natural wood fibers are an excellent filler for PLA as both are composable and affordable, lowering the overall cost of the product while maintaining biodegradability [14]. The rheological properties of wood fiber-filled PLA were studied in terms of temperature and wood fiber filler concentration [15]. A 3D printing filament developed from 5% cork-reinforced PLA composite was successfully used for FDM application, which showed that, except for elongation at break, where 3D-printed composite was more ductile than compression-molded composites, the mechanical characteristics of the 3D-printed composite were slightly decreased [16]. The mechanical characteristics of carbon fiber–reinforced polylactic acid composite were studied by changing FDM parameters such as layer thickness, raster angle, infill density, and printing speed [17]. The primary objective of the research was to use the newly developed PLA filament reinforced with 25 wt% *Acacia concinna* filler (ACF) in the FDM process and optimize the process parameters. The tensile, flexural, and impact strength were evaluated in the FDM-fabricated composite specimens, and the tensile fracture morphology was studied.

Kristiawan et al. [19] investigated the various parameters that were responsible for affecting the mechanical properties and reported that the following factors filament material composition, extrusion working parameters such as those related to extrusion speed and temperature, FDM machine specifications, extrusion machine specifications, type of filament polymer, and FDM work parameters when printing the filament. Polymer filament-based 3D printing has been used to identify the additive manufacturing field's potential for future research in optimizing FDM methods and materials. It has been stressed that the quality of the products and the mechanical qualities of FDM are both influenced by a large number of process parameters. Some of the relationships between variables and factors are still not fully understood; therefore, further research is needed to get a better idea of how to proceed.

Singh et al. [18] explored the usage of recycled materials for energy storage materials as a dry cell using additive manufacturing techniques. He used the material comprises

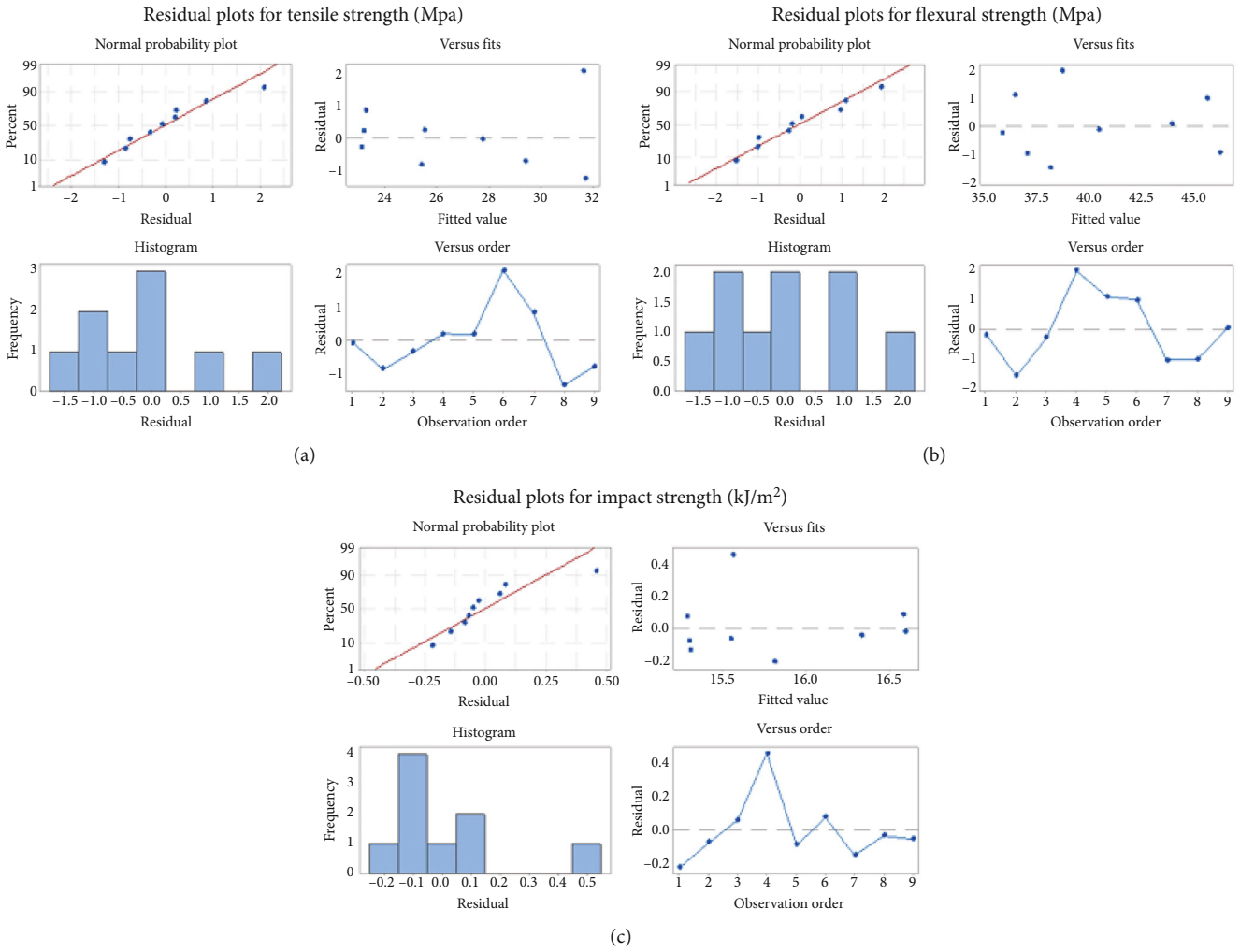

Figure 4: Residual plots for (a) tensile strength, (b) flexural strength, and (c) impact strength.

of ABS matrix, reinforced with different proportions of chemicals/salts, namely MnO_2, $ZnCl_2$, NH_4Cl, and graphite. This work shows that using the proposed technology, dry cells made up of at least 40% recycled thermoplastics can be effectively manufactured, with voltage potentials comparable to commercial dry cells.

2. Materials and Methods

2.1. Materials. Polyvinyl alcohol was supplied by Sigma-Aldrich Chemicals Private Limited, Bengaluru, India (Figure 1(a)). *A. concinna* (*Senegalia rugata*) was collected from Sathuragiri Forest, Madurai district, Tamil Nadu, India (Figure 1(b)). The collected *A. concinna* was cleaned and soaked in distilled water for 24 h. Impurities and foreign particles were detached from *A. concinna* by the soaking process, and *A. concinna* was allowed to dry under the sunlight for 3 days to remove the moisture content. Furthermore, it was kept in a vacuum air oven at 80°C for 5 h. Then, the dried *A. concinna* was powdered by a mechanical pulverizer at 350 rpm for 60 min and the chamber was allowed to cool every 5 min. Figure 1(c) shows the pulverized ACF. Figure 1(d) shows the particle size of the ACF. The particle size of the ACF was less than 10 μm, measured using a particle size analyzer.

2.2. Filament Compounding. Before compounding, the PLA granules and ACFs were dried at 80°C for 5 h in an air-circulated oven and then they were dry mixed. The dry-mixed PLA granules (75 wt%) and ACFs (25 wt%) were extrudate in a single-screw extruder incorporated with feed hopper mixing. Throughout the process, the extrusion speed was maintained at 20 mm/s. The average temperature maintained for the feed zone to the die of the extruder was 160°C. The extrudate from the die of diameter 1.75 mm (Figure 2(a)) was quenched in a water tank at 20–30°C and then wounded using a winding mechanism.

2.3. Fabrication of Composite Samples Using Fused Deposition Modelling. In this study, the FlashForge Finder 3D printer with a built volume of $200 \times 200 \times 200 mm^3$ was used. This printer has a standard nozzle of diameter 0.4 mm, layer thickness (Z resolution) of 0.05–0.4 mm, maximum build speed of 100 mm/s, and maximum extruder

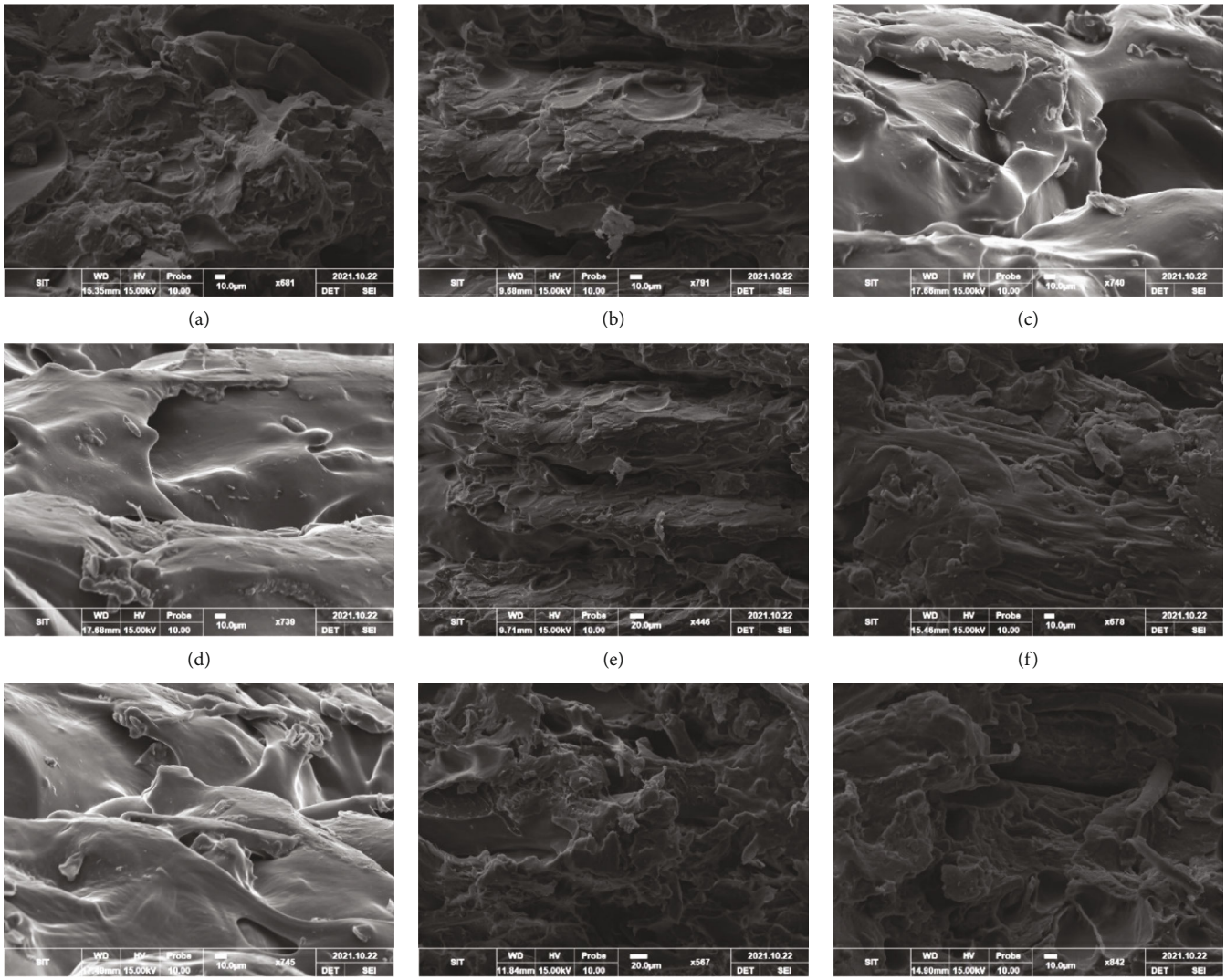

Figure 5: Micrographs of tensile fractography according to Table 2.

temperature of 260°C. Polylactic acid reinforced with 25% ACF was used in this study. The composite samples were prepared as per the ASTM standards and details are shown in Table 1. Other parameters such as build orientation of 0° and nozzle temperature of 200°C were maintained at a constant level.

2.4. Experimental Procedures. In this study, response surface methodology (RSM), a statistical method to model and optimize the FDM process parameters, was used. Nine experiments (L9) were planned and three input factors, namely layer thickness, infill density, and printing speed, were taken into consideration for optimizing the FDM process. Each input control factor analyzed at three levels is shown in Table 1. Figure 2(b) shows the printed PLA/ACF composite test specimens according to the input parameters. The range of these variables was determined by conducting many pilot experiments by varying one factor at a time. Tensile, flexural, and impact strength were taken as the output responses of experimental analysis. The empirical models were developed using statistical multiple regression analysis.

2.5. Testing of Mechanical and Properties. A flat printed specimen with 100 mm × 20 mm × 8 mm was used for the tensile tests, which were conducted in accordance with ASTM Standard D 3039. The test was carried out in a servo-controlled computerized universal testing machine (UTM) with a constant strain rate of 1×10^{-4} m/s. The flexural test was conducted in the servo-controlled UTM using a three-point loading setup according to ASTM Standard D 7264 with a size of 220 mm length × 20 mm width × 10 mm thickness. The Charpy impact test was performed as per ASTM Standard D 256.

3. Results and Discussion

3.1. Analysis of Mechanical Properties. The specimens prepared from the PLA/AC filament were subjected to tensile, flexural, and impact tests, and the results obtained are listed

in Table 2. Figures 3(a)–3(c) shows the effect of input control factors on tensile, flexural, and impact strength of PLA/AC composites. It is seen that an increase in the layer height and infill percentage results in an increase in the mechanical strength. This may be because the increased material deposition contributes to achieve a better mechanical strength [4, 16]. However, an increase in the printing speed results in a reduction in the tensile, flexural, and impact strength because a high-printing-speed specimen may release the bonding of adjacent layers.

3.2. Analysis of Variance. Tables 3–5 show the results of the analysis of variance (ANOVA) for the tensile, flexural, and impact strength of the composites, respectively. Factors layer height (mm) and print speed (mm/s) are significant as their p-value is less than 0.05 for tensile, flexural, and impact strength. The percentage contribution of the input control factors was calculated by dividing the sum of squares of a factor by the total sum of squares. The percentage contribution values of the control factors are specified in the last column of Tables 3–5. On the basis of ANOVA results, it was found that printing speed contribution was maximum, followed by layer height and infill percentage.

3.3. Mathematical Modeling and Prediction. The mathematical expression of tensile, flexural, and impact strength for the composites is shown below. The regression equations are the following:

Tensile strength (MPa) = 31.65 + 16.98 layer height (mm) + 0.0629 infill percentage − 0.1805 print speed (mm/s);

Flexural strength (MPa) = 43.23 + 26.65 layer height (mm) + 0.0774 infill percentage − 0.1919 print speed (mm/s);

Impact strength (kJ/m^2) = 16.082 + 3.31 layer height (mm) + 0.01277 infill percentage − 0.02599 print speed (mm/s).

The normal probability plot was used to determine the adequacy of the model developed. Figures 4(a)–4(c) displays the normal probability plot of the residuals for the PLA/AC composites for tensile, flexural, and impact strength. The residuals are found to be adjacent to the normal probability line, which confirms that the developed model is adequate. Also, Figures 4(a)–4(c) indicates that the errors are spread out in a regular manner. The residual plot shows that all the run residues lay at the acceptable levels.

From the experimental results, it is evident that the composite sample 6 showed a better mechanical strength than the other samples. Because sample 6 is printed with a nominal layer height of 0.16 mm, maximum infill density of 100%, and minimum printing speed of 50 mm/s, it resulted in a better mechanical strength. Under this condition, the sample was printed with minimum voids in the internal regions and also low printing speed provided the even distribution of the material along its length.

3.4. Fracture Morphology. Figure 5 shows the micrographs of the tensile fractured samples for the fabricated specimens reported in Table 2. It is noted that all the fracture samples have a ductile fracture with the uniformly distributed structure. Figures 5(c), 5(d), and 5(g) shows the maximum mode of fracture and the corresponding samples are low tensile strength (Table 2). Figures 5(f) and 5(h) shows the minimum mode of fracture than other micrographs.

4. Conclusion

The newly developed PLA filament consisting 25 wt% ACF was successfully used in the FDM process by varying the layer thickness, infill density, and printing speed. Mechanical characteristics of the FDM-fabricated PLA/AC composites were analyzed and the following conclusions were made:

(i) The mechanical strength was enhanced in the PLA/25 wt% *A. concinna* composite specimen compared with the pure PLA specimen for the all-input control parameters.

(ii) ANOVA showed that the printing speed is the most significant control factor that have 73.04%, 62.92%, and 59.19% contribution to tensile, flexural, and impact strength of composites, respectively. Layer height has 10.34%, 19.40%, and 15.35% contribution to tensile, flexural, and impact strength of composites, respectively.

(iii) Infill percentage has 8.87%, 10.23%, and 14.29% contribution to tensile, flexural, and impact strength of composites, respectively.

(iv) The mathematical model was developed using multiple linear regression analysis, and residual plots confirmed that the model was adequate.

(v) Overall results depicted that the printing speed is the predominant control factor that affects the tensile, flexural, and impact strength of the composites.

(vi) The micrographs of the tensile fractography confirmed the ductile mode of the fracture.

(vii) It is concluded that layer height of 0.16 mm, 100% infill percentage, and print speed of 50 mm/s are better FDM control factor levels for PLA/AC composites.

Data Availability

There is no data availability statement.

Conflicts of Interest

The authors declare that they have no conflicts of interest.

References

[1] T. D. Ngo, A. Kashani, G. Imbalzano, K. T. Q. Nguyen, and D. Hui, "Additive manufacturing (3D printing): a review of materials, methods, applications and challenges," *Composites Part B: Engineering*, vol. 143, pp. 172–196, 2018.

[2] J. Justo, L. Távara, L. García-Guzmán, and F. París, "Characterization of 3D printed long fibre reinforced composites," *Composite Structures*, vol. 185, pp. 537–548, 2018.

[3] V. Shanmugam, D. J. J. Rajendran, K. Babu et al., "The mechanical testing and performance analysis of polymer-fibre composites prepared through the additive manufacturing," *Polymer Testing*, vol. 93, article 106925, 2021.

[4] X. Song, W. He, P. Chen, Q. Wei, J. Wen, and G. Xiao, "Fused deposition modeling of poly (lactic acid)/almond shell composite filaments," *Polymer Composites*, vol. 42, no. 2, pp. 899–913, 2021.

[5] F. Ning, W. Cong, J. Qiu, J. Wei, and S. Wang, "Additive manufacturing of carbon fiber reinforced thermoplastic composites using fused deposition modeling," *Composites Part B: Engineering*, vol. 80, pp. 369–378, 2015.

[6] R. van Wassenhove, L. De Laet, and A. P. Vassilopoulos, "A 3D printed bio-composite removable connection system for bamboo spatial structures," *Composite Structures*, vol. 269, article 114047, 2021.

[7] B. Brenken, E. Barocio, A. Favaloro, V. Kunc, and R. B. Pipes, "Development and validation of extrusion deposition additive manufacturing process simulations," *Additive Manufacturing*, vol. 25, pp. 218–226, 2019.

[8] N. Kumar, P. K. Jain, P. Tandon, and P. M. Pandey, "The effect of process parameters on tensile behavior of 3D printed flexible parts of ethylene vinyl acetate (EVA)," *Journal of Manufacturing Processes*, vol. 35, no. 35, pp. 317–326, 2018.

[9] N. Krajangsawasdi, L. G. Blok, I. Hamerton, M. L. Longana, B. K. S. Woods, and D. S. Ivanov, "Fused deposition modelling of fibre reinforced polymer composites: a parametric review," *Journal of Composites Science*, vol. 5, no. 1, p. 29, 2021.

[10] S. S. Nair and N. Yan, "Bark derived submicron-sized and nano-sized cellulose fibers: from industrial waste to high performance materials," *Carbohydrate Polymers*, vol. 134, pp. 258–266, 2015.

[11] R. T. L. Ferreira, I. C. Amatte, T. A. Dutra, and D. Bürger, "Experimental characterization and micrography of 3D printed PLA and PLA reinforced with short carbon fibers," *Composites Part B: Engineering*, vol. 124, pp. 88–100, 2017.

[12] V. Mazzanti, L. Malagutti, and F. Mollica, "FDM 3D printing of polymers containing natural fillers: a review of their mechanical properties," *Polymers*, vol. 11, no. 7, p. 1094, 2019.

[13] M. A. Osman and M. R. Atia, "Investigation of ABS-rice straw composite feedstock filament for FDM," *Rapid Prototyping Journal*, vol. 24, no. 6, pp. 1067–1075, 2018.

[14] S. Kumar, R. Singh, T. P. Singh, and A. Batish, "On mechanical characterization of 3-D printed PLA-PVC-wood dust-Fe_3O_4 composite," *Journal of Thermoplastic Composite Materials*, vol. 35, no. 1, pp. 36–53, 2022.

[15] V. Mazzanti and F. Mollica, "Rheological behavior of wood flour filled poly (lactic acid): temperature and concentration dependence," *Polymer Composites*, vol. 40, no. S1, pp. E169–E176, 2019.

[16] F. Daver, K. P. M. Lee, M. Brandt, and R. Shanks, "Cork-PLA composite filaments for fused deposition modelling," *Composites Science and Technology*, vol. 168, pp. 230–237, 2018.

[17] K. R. Kumar, V. Mohanavel, and K. Kiran, "Mechanical properties and characterization of Polylactic acid/carbon fiber composite fabricated by fused deposition modeling," *Journal of Materials Engineering and Performance*, vol. 31, no. 6, pp. 4877–4886, 2022.

[18] R. Singh, H. Singh, I. Farina, F. Colangelo, and F. Fraternali, "On the additive manufacturing of an energy storage device from recycled material," *Composites Part B: Engineering*, vol. 156, pp. 259–265, 2019.

[19] R. B. Kristiawan, F. Imaduddin, D. Ariawan, and Z. Arifin, "A review on the fused deposition modeling (FDM) 3D printing: filament processing, materials, and printing parameters," *Open Engineering*, vol. 11, no. 1, pp. 639–649, 2021.